Journal of Ceramic Processing Research. Vol. 23, No. 2, pp. 158~164 (2022)
(Received 28 August 2021, Received in revised form 25 November 2021, Accepted 27 November 2021)
https://doi.org/10.36410/jcpr.2022.23.2.158

J O U R N A L O F
Ceramic Processing Research

Irradiation time-dependent study of eggshell-derived hydroxyapatite powder synthesized by microwave-assisted wet chemical precipitation method

K.W. Goh[a], Y.H. Wong[a], R.S.K. Singh[a,b], Hari Chandran[c], S.K. Wong[d] and K.Y. Sara Lee[e,*]
[a]Faculty of Engineering, University of Malaya, 50603 Kuala Lumpur, Malaysia
[b]Faculty of Engineering, Universiti Teknologi Brunei, Tungku Highway, Gadong BE1410, Brunei Darussalam
[c]Division of Neurosurgery, Faculty of Medicine, University of Malaya, 50603 Kuala Lumpur, Malaysia
[d]Department of Pharmacology, Faculty of Medicine, Universiti Kebangsaan Malaysia, Jalan Yaacob Latif, Bandar Tun Razak, 56000 Cheras, Kuala Lumpur, Malaysia
[e]Tunku Abdul Rahman University College, Faculty of Engineering & Technology, Department of Mechanical Engineering, 53300, Kuala Lumpur, Malaysia

The extraction of calcium from natural biowaste material such as chicken eggshells have been shown to be viable to synthesis calcium phosphate bioceramic. In this work, eggshell-derived hydroxyapatite powder was synthesised by using the wet chemical precipitation technique coupled with microwave irradiation at low power (700 W) at varying exposure time from 5 to 30 min. The derived nano-powders were examined to determine the phases present, chemical bonding and microstructural evolution. It was revealed that the irradiation time has an effect on the degree of crystallinity and both the crystallite and particle size of the derived powders although the hydroxyapatite phase stability was not disrupted. An exposure time of 15 min. was determined to be sufficient when subjected to low power microwave irradiation to formed a well-defined needle-like hydroxyapatite particles having an average crystallite size of about 22 nm. On the contrary to many literatures, this study has demonstrated the viability of synthesizing a useful bioceramic from using biowaste eggshells coupled with microwave irradiation at low power of 700 W for very short period of time to produce nano-range needle-like hydroxyapatite particles suitable for biomedical application.

Keywords: Eggshells, Calcium phosphate, Bioceramic, Microwave-assisted synthesis, Hydroxyapatite.

Introduction

There has been a tremendous interest over the past 10 years in the development of calcium phosphate (CaP) family for a host of clinical applications [1-14]. CaPs were extensively used as biomaterials for bone replacement, and as a coating material for metallic prostheses [15-19]. Besides this material, other bioceramics such as tetragonal zirconia polycrystals and alumina-based biocomposite have also received great attention for use as either a bioinert or bioactive biomaterials [20-35]. In all these studies, it has been shown that the properties of the bioceramics could be tailored to suit a particular application through the control of processing parameters and microstructure.

CaP based on hydroxyapatite (HA, $Ca_{10}(PO_4)_6(OH)_2$) is a widely accepted bioceramic for bone substitute among the CaP family members, because it is the major inorganic component found in human bones [36-40]. In general, human bones is composed of about 70 wt % of HA, 22 wt % of protein and 8 wt % of water [41, 42]. HA is biologically and chemically similar with human native tissue as well as its crystallographic structure. In addition, HA comprises excellent osteoconductivity [43], biocompatibility [42] and bioactivity [44] properties. It provides a stable bio-resorption at the interface result in formation of a strong bonding between the HA particles and bone tissues. This helps in enhancing the implant fixation without any physiological effect on human beings.

Over the past years, several studies have reported on the preparation of HA (Ca/P ratio = 1.67) powder derived from various inexpensive natural materials such as eggshells [10, 11], fish bones [47], sheep bone [7], pig bone [48] and bovine bone [49-51]. Among the aforementioned, eggshell is one of the natural biowaste materials which provides the most sources of calcium, consisting of 94% of calcium carbonate [52], 4% of organic matter [53], 1% of calcium phosphate [54], and 1% of magnesium carbonate [55]. Moreover, the eggshell itself represents 11% of the total weight of the chicken egg which is about 60 g. It is an established fact that about million tons of chicken eggshells are discarded as waste from industries everyday across the globe. According to the 2017 report from the Feder-

*Corresponding author:
Tel : +(6)03-41450123
Fax: +(6)03-41423166
E-mail: leeky@tarc.edu.my

ation of Livestock Farmer's Associations of Malaysia (FLFAM), Malaysia alone has produced approximately 12.5 billion of chicken eggs from about 257 local farms. These biowaste eggshells could facilitate microbial activities which may contribute to environmental pollution. Thus, the recycling of the eggshells as a potential source of calcium for the production of calcium phosphate bioceramics could be explored.

Numerous attempts have been made to recycle chicken eggshells into useful product for biomedical purposes with the aim of enhancing the HA characteristics with lower processing cost [52, 56]. Kang et al. [57] prepared submicron size of needle-like HA particles using eggshells and H_3PO_4 via the mechanochemical method. Naga et al. [58] synthesized the nanosized particles of HA powder from eggshells and H_3PO_4 via the wet precipitation method. A spherical like HA powder with micron size had been produced also from eggshells and dicalcium phosphate dihydrate (DCPD) by Ho et al. [53] using the mechanochemical method. These studies revealed that the preparation of HA powder was strongly dependent on the different powder processing methods employed, including the chemicals (raw materials and reagents used) as well as the synthesis parameters (pH, heating time and temperature) [41]. Thus, the combination of different chemical and synthesis parameters will result in the formation of different characteristics of HA powder.

There are a variety of techniques which have been used in synthesizing HA nanostructure with different morphologies from eggshells using direct or indirect conversion methods [59]. Direct conversion method can be accomplished via the hydrothermal method [60] whereas the indirect method is done by formation of calcium precursors from eggshells as the first step, which is followed by HA preparation via several methods such as sol-gel [61], mechanochemical [62, 63] and wet precipitation [45, 46, 64] as the second step. However, the synthesis of HA powder by approaching any of these methods has been reported to have suffered from drawbacks, including powder agglomeration [1, 5], complex synthesis process [65] and long reaction times [66]. In addition, it should be noted that natural bone consists of HA nanoparticles in the form of needle-like and rod-like shapes with length of 10 to 80 nm [41]. Nano-sized HA have more advantages than micron-sized HA in the osteoblast activities [41, 43]. Thus, the formation of nano HA is vital since large surface area of small crystals make them very active and their properties may alter accordingly [67]. In other word, the performance of HA bioceramic with excellent mechanical properties based on reports from literature, is highly dependent on the structural properties of starting stoichiometric HA powder in terms of the particle size, morphology, and particle distribution [43]. Therefore, it is necessary to design a simple and effective processing method that is able to control and improve the HA powder properties [66].

Recently, microwave-assisted method was used to synthesize pure HA [68]. Microwave-assisted offers rapid heating rate [69], fast chemical reactions [70], high crystallinity [71], high purity [72], and narrow particle distribution [73]. Wang and Fu [65] synthesized HA powders using $Ca(NO_3)_2.4H_2O$, H_3PO_4 and EDTA as raw materials via the microwave-hydrothermal method in the temperature range between 100 °C to 140 °C. They found that highly crystalline HA nano particles with an average crystallite size of 54.7 nm could be obtained at 140 °C after only 1 min. of microwave treatment. Kumar et al. [52] successfully produced flower-like HA nano particles using eggshells as the based material via the microwave-wet precipitation method with the aid of EDTA as a chelating agent. The reaction mixture was only irradiated for 10 min. at 600 W. In addition, it is worth noting that the growth of intermediate metastable phases like tricalcium phosphates (TCP) could be avoided due to the rapid heating process and fast crystallization rate, which favours the formation of the stable phase [65, 74].

In general, the characteristics of the HA particles produced via microwave-assisted method are influence by the processing parameters including the type of precursors used [74], concentration of the mixture [70, 75], heating temperature [65], and irradiation time [76-78]. Although, the effect of precursors, microwave power and irradiation time have been studied and optimized, in most cases this was accomplished by using expensive raw material, higher power input or longer irradiation time. Up to date, the synthesis of HA powder from eggshells via the microwave-assisted method have not been fully explored. Thus, in this work, we explore the possibility of producing a stoichiometric eggshell-derived HA nano particles by using the shortest possible irradiation time at low microwave power of 700 W. It is envisaged that the synthesis HA would possess superior physical and mechanical properties suitable for use in clinical application either as a solid implant, fillers, scaffold, porous implant and as coatings on metallic implants.

Experimental Procedure

In the present study, the chicken eggshells, orthophosphoric acid (H_3PO_4) and ammonia hydroxide (NH_4OH) were used as starting materials. The chicken eggshells were initially cleaned in boiling water to remove contaminants and the inner membrane. The cleaned chicken eggshells were then dried overnight in oven at 80 °C and then grounded into powder form using mortar and pestle. The produced brown eggshell powders were sieved through a 212 mm mesh sieve and calcined in a furnace at 900 °C for 1 h using a heating rate of 10 °C/min. [76]. This heating parameters were selected based on previous work [56, 76] which

showed that the brown eggshell powders ($CaCO_3$) which composed purely of calcium carbonate ($CaCO_3$) decomposed completely to form a white calcium oxide (CaO) powder as shown in Fig. 1.

The HA powder was synthesised based on a Ca/P ratio of 1.67. In a typical mixture, the required amounts of CaO powder and H_3PO_4 were measured and dissolve in distilled water under constant stirring for 15 min. The H_3PO_4 solution was then added dropwise into the calcium precursor. The pH value of the mixture was monitored and adjusted to maintain it at 10 by the addition of appropriate amount of NH_4OH solution [76]. The mixture was then irradiated in a Panasonic microwave (MW) oven (700 W) at different MW-irradiation times of 5, 10, 15, 20 and 30 min. The obtained precipitate was washed using distilled water and then dried to obtained the HA powders.

The crystal phase composition of the synthesized HA samples was determined using PANalytical Empyrean X-ray Diffractometer (XRD) in the range of 20° to 80° with CuKα as the radiation source. The functional groups of the HA samples were identified by using a Perkin Elmer Spectrum 400 Fourier transform infrared spectroscopy (FTIR) over the region 650 to 4000 cm^{-1}. A Carl Zeiss Auriga field emission scanning electron microscope (FESEM) coupled with an energy dispersive X-ray spectroscopy (EDX) was used to examine the morphology of the particles and to identify the elemental composition of the samples.

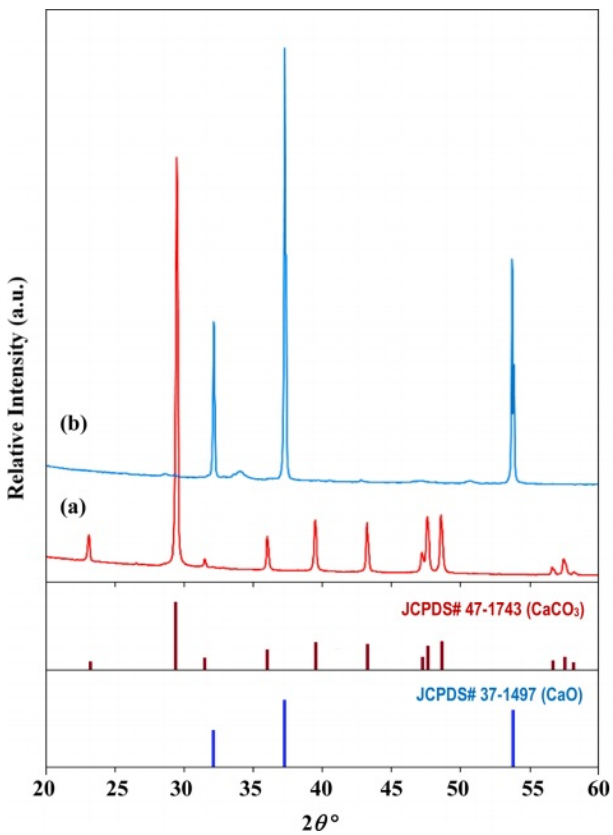

Fig. 1. X-ray diffraction pattern of (a) the starting eggshells which comprised mainly of $CaCO_3$ and (b) the resulting powder obtained after calcination at 900 °C which composed of pure CaO [56].

Results and Discussion

The XRD analysis of the synthesized HA powder at different MW-irradiation times are shown in Fig. 2. All the peaks compared very favourably to that of the Miller's planes of hexagonal HA phase (JCPDS No. 09-0432). Secondary phases such as α-TCP, β-TCP, $CaCO_3$, and CaO were not detected in all the samples thus indicating the successful conversion of the CaO to a stable HA was accomplished via microwave irradiation. In addition, the crystallinity of the powder was observed to improve with increasing irradiation time from 5 to 30 min. as evident from the increasing intensity of the HA peaks and decreasing peak width. This improvement could be associated with the rapid volumetric heating imposed by the microwave energy [41, 79]. Yang et al.

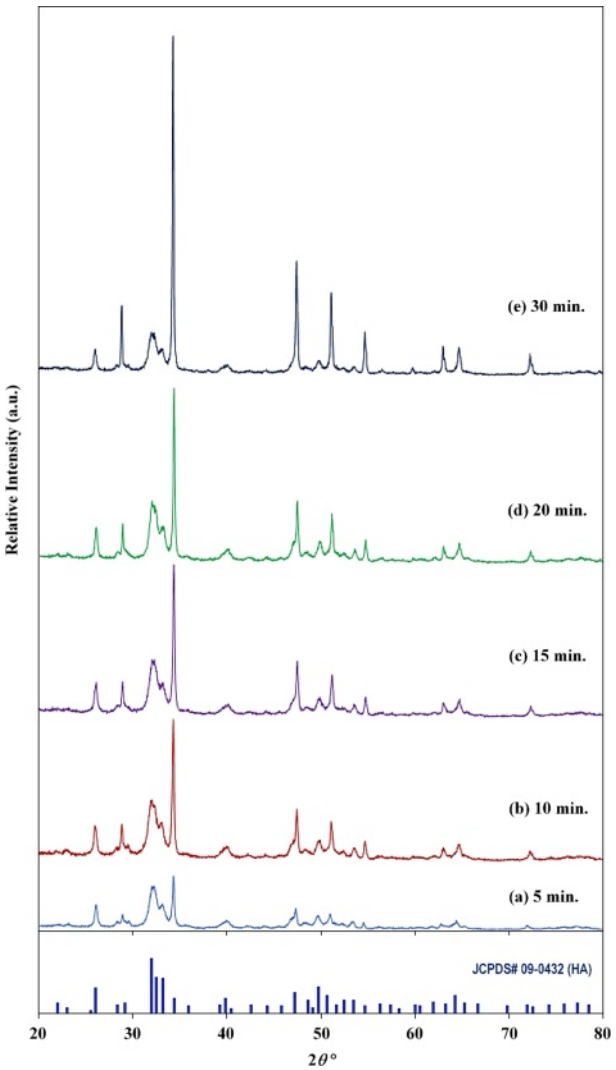

Fig. 2. XRD patterns of HA powders subjected to microwave irradiation from 5 to 30 mins.

[78] reported that HA powder could be formed via microwave heating above 700 W. Singh et al. [66] supported this observation and they reported that the stability of the HA phases was not disrupted as the microwave power increased from 900 W to 1200 W. Similarly, Nazir et al. [79] found that the crystallinity of HA powder gradually increased as the microwave power increased from 600 W to 1000 W. However, in the present work, increasing the MW power was not necessary as the crystallinity improved with increasing the irradiation time.

The average crystallite size (D) of the HA powder was estimated using Scherrer's formula as given in Eq. (1) [41, 66].

$$D = 0.9\lambda / \beta \cos\theta \quad (1)$$

where λ is the wavelength of the X-ray radiation used (0.154 nm), β is the full width at half maximum and θ is the peak position. In this experiment, all the main peaks of HA were used to determine the average crystallite size. It was found that the average crystallite size of the HA powders varies according to MW-irradiation time as follows: 40.7 nm, 28.0 nm, 22.0 nm, 24.2 nm and 28.3 nm for 5, 10, 15, 20 and 30 min., respectively. Initially, the average crystallite size decreased with increasing irradiation time and reached a minimum of 22 nm at 15 min. before increasing with further increased in irradiation time, believed to be due to coarsening and to some extent, agglomeration of the HA crystals.

For comparison purpose, the average crystallite size of all the samples was also evaluated using the Williamson-Hall (W-H) equation by associating the microstrain (ε) produced in the powder due to imperfection based on the relationship shown in Eq. (2) [80, 81].

$$\beta \cos\theta = 4\varepsilon \sin\theta + \frac{K\lambda}{D} \quad (2)$$

Comparing Eq. (2) with the standard equation for a linear line graph (i.e. $y = mx + c$), the plot $\beta\cos\theta$ versus 4 sin θ will produce a graph in which the gradient of the linear fit will give the microstrain and the crystallite size can be obtained from the y-intercept [76, 82]. This plot was made for all the samples as shown in Fig. 3. Five points with goodness fit (R^2) of all samples between 0.907 and 0.977 were selected from the distribution values and the crystallite size was determined. The results showed that the crystallite size based on the W-H equation decreased from 14.6 nm to 3.7 nm as the irradiation time increased from 5 min. to 15 min. Thereafter, the crystallite started to increase, reaching 20.5 nm for the 30 min. irradiation. It is expected that both equations would produce different crystallite sizes, however in both cases, a similar crystallite size variation trend with increasing irradiation time was observed as shown in Fig. 4. In both calculations, the HA powder which was irradiated for 15 min. exhibited the smallest crystallite size. Owing to the rapid and volumetric heating achieved via microwave processing, this would induce localised hot spots that promotes the nucleation of crystals [83]. It is envisaged that a short irradiation time of less than 15 min. could not have introduced as many nucleation sites for crystals to grow simultaneously thus resulting in the agglomeration of larger crystallites. On the other hand, longer exposure time, above 15 min., could have accelerated that the growth kinetics thus promoting coarsening of the crystals. The 15 min. irradiation time seemed to be the optimum exposure time required to promote the nucleation process and formation of small crystals. Sabu et al. [83] and Jhung et al. [84] reported that the microwave heating has more effect on the nucleation rate of the crystals when compared to the rate of crystal growth. However, the mechanism responsible for enhancing the nucleation rate with microwave heating is still a subject of debate.

The FTIR spectrum of the synthesized HA powder at different irradiation times is shown in Fig. 5. The presence of phosphate (PO_4^{3-}), carbonate (CO_3^{2-}) and hydroxide (OH^-) ions were observed in all of the HA powders.

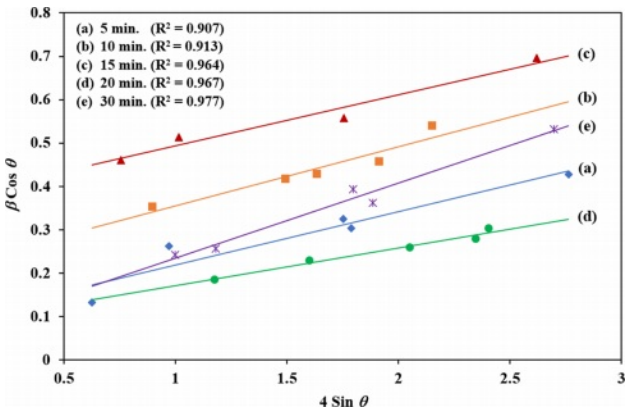

Fig. 3. The W-H plot of synthesized HA powder for different MW irradiation times.

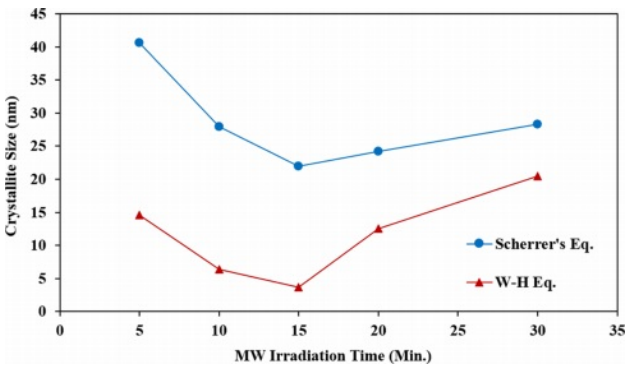

Fig. 4. Crystallite size of HA determined from Scherrer's and W-H equations.

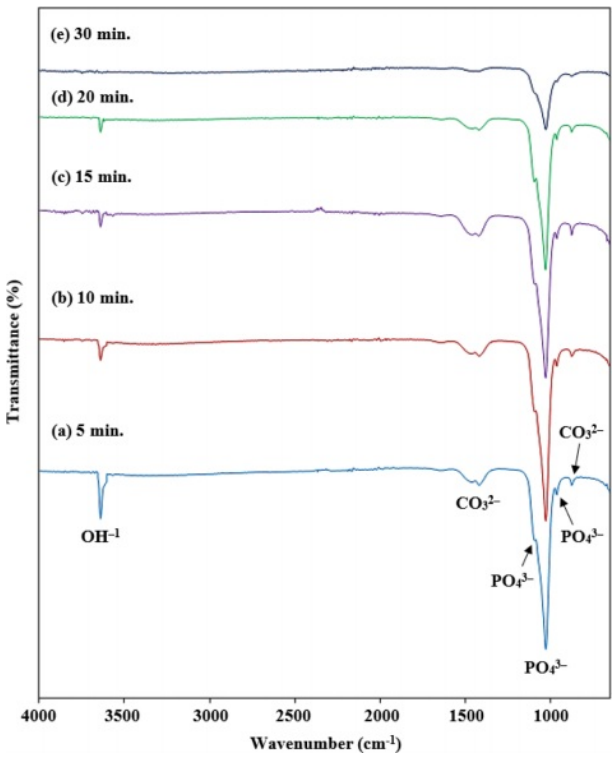

Fig. 5. FTIR spectrum of HA powder at different MW-irradiation time.

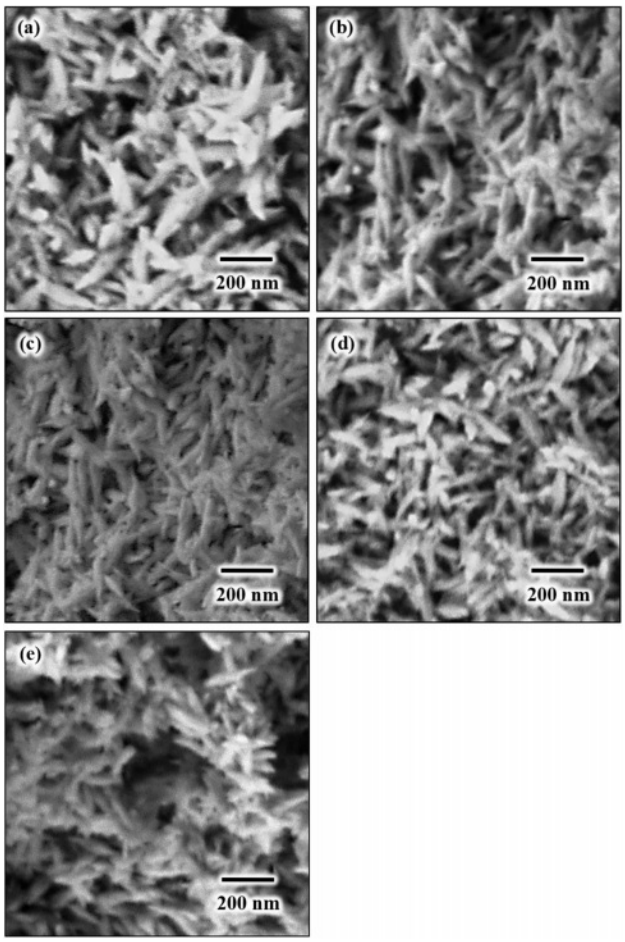

Fig. 6. FESEM images of MW-irradiated HA powders taken at high magnification of ´50,000 revealing needle-like nano particles regardless of irradiation time: (a) 5 min, (b) 10 min., (c) 15 min., (d) 20 min. and (e) 30 min.

The band observed at 1100 cm^{-1}, 1031 cm^{-1} and 962 cm^{-1} in all the samples were assigned to the asymmetric stretching and bending vibrations mode of P-O bond in the PO_4^{3-} group [76]. The band observed at 1100 cm^{-1} and 1031 cm^{-1} were correspondent to the stretching vibration (v_3) whereas the band at 962 cm^{-1} can be attributed to the bending modes (v_1) of the PO_4^{3-} group [52, 76]. These characteristics of the PO_4^{3-} vibrations confirmed the formation of the HA phase [52, 83]. Additionally, a small band of CO_3^{2-} can be seen at 1445 cm^{-1} and 870 cm^{-1} which ascribed to the C-O stretching of the CO_3^{2-} group in the HA sample [85]. This may have arisen due to the entrapment of atmospheric carbon dioxide in the HA crystal structure which replaced the phosphate group during the synthesis process [41, 85]. However, the inclusion of a small amount of CO_3^{2-} ion did not affect the HA phase. No other carbonates substituted HA was detected in the FTIR analysis. This result is in good agreement with the XRD analysis. The weak band at 3634 cm^{-1} is related to the O-H stretching mode of the hydroxyl group [86]. It can be seen that the peak at 3634 cm^{-1} decreases in accordance to an increased in the irradiation time. It can be assumed that very little portion of water molecules is retained in the HA lattice after 15 min. of microwave.

The FESEM images of HA powders after microwave irradiation for 15 min. is shown in Fig. 6. In general, all the powders exhibited a needle-like shape particles of nano crystallites HA regardless of irradiation time. The agglomeration of the HA particles was inevitable regardless of heating time due mainly to the formation of a short-range surface forces such as van der Waals and hydrophilicity [87]. It can be anticipated that there will be some OH remaining in the lattice after the microwave irradiation as evident from the FTIR analysis. During heating, the microwave energy enabled a rapid absorption of water molecules in the sphere of a polyvalent ion hydration. The microwave energy that is absorbed by bound water will diminish the strength of the bonds between the calcium (Ca) ions and its sphere of hydration. This reaction is very important as it is the pre-requisites for the formation of HA particles in aqueous solution [69, 73].

It is noteworthy that the needle-like HA powder can improve the fracture toughness of medical implants [45, 88]. Thus, similar needle-like morphology of HA has also been prepared from eggshells by many researchers as reported in literatures. For example, Kamalanathan et al. [45] successfully synthesised a needle-like HA powder from eggshells via wet chemical precipitation. The obtained HA suspension was permitted to mature for 24 h and was subsequently filtered and dried at 60

°C in an oven for 24 h. In another research, Wu et al. [60] used a hydrothermal method to produce a needle-like HA powder from eggshells and fruit wastes. The precursor was sealed in polytetrafluoroethylene (Teflon)-lined stainless-steel autoclaves and heated at 150 °C for 24 h. The HA particle was agglomerated with a length around 100 nm. Apalangya et al. [77] synthesized eggshell-derived HA particles via microwave-assisted mechanochemical method. They reported that a stoichiometric HA particle (crystallite size about 70 nm) was only obtained after irradiated for 30 min. In all these studies a long reaction times and/or complex processes were required to synthesis a needle-like HA powder which was not the case in the present work.

Conclusions

In the present work, nano-crystalline HA needle-like particles were successfully synthesized from eggshells by using a simple wet chemical precipitation method followed by microwave irradiation in a domestic microwave oven at 700 W for a short period of time. The phase analysis indicated that the final powders composed of pure hexagonal HA regardless of irradiation time. This was also confirmed by FTIR which exhibited the formation of the Ca, PO and OH functional groups belonging to hydroxyapatite. A microwave-irradiation time of 15 min. was found to be optimum for the formation of needle-like particles having fine HA crystallites using biowaste eggshells as the calcium precursor.

Acknowledgements

This research was supported under the FRGS grant no. FP020-2018A.

References

1. A.A. Al-allaq, J.S. Kashan, M.T. El-Wakad, and A.M. Soliman, J. Ceram. Process. Res. 22 (2021) 446-454.
2. S.A. Doğdu, C. Turan, T. Depci, and D. Ayas, J. Ceram. Process. Res. 22 (2021) 356-361.
3. N.A.M. Radzuan, A.B. Sulong, F.M. Foudzi, M.Y. Zakaria, and M.I. Ramli, J. Ceram. Process. Res. 21 (2020) 662-666.
4. S. Pazarlioglu and S. Salman, J. Ceram. Process. Res. 20 (2019) 99-112.
5. S. Ramesh, C.J. Gan, L.T. Bang, A. Niakan, C.Y. Tan, J. Purbolaksono, H. Chandran, S. Ramesh, B.K. Yap, and W.D. Teng, J. Ceram. Process. Res. 16 (2015) 683-689.
6. J.-H. Lim, C.-K. Park, C.-H. Jin, S.-Y. Beck, and D.-Y. Jeong, J. Ceram. Process. Res. 18 (2017) 404-408.
7. N. Ekrena, J. Ceram. Process. Res. 18 (2017) 64-68.
8. S. Ramesh, C. Gill, and S. Lawson, J. Mater. Sci. 34 (1999) 5457-5467.
9. I. Sopyan, S. Ramesh, N.A. Nawawi, A. Tampieri, and S. Sprio, Ceram. Int. 37 (2011) 3703-3715.
10. L.T. Bang, S. Ramesh, J. Purbolaksono, Y.C. Ching, B.D. Long, Hari Chandran, S. Ramesh, and R. Othman, Mater. Des. 87 (2015) 788-796.
11. S. Ramesh, A. Yaghoubi, K.Y. Sara Lee, K.M. Christopher Chin, J. Purbolaksono, M. Hamdi, and M.A. Hassan, J. Mech. Behav. Biomed. Mater. 25 (2013) 63-69.
12. S. Ramesh, C.Y. Tan, R. Tolouei, M. Amiriyan, J. Purbolaksono, I. Sopyan, and W.D. Teng, Mater. Des. 34 (2012) 148-154.
13. I. Sopyan, R. Singh, and M. Hamdi, Indian J. Chem. 47A (2008) 1626-1631.
14. S. Ramesh, S. Meenaloshini, C. Y. Tan, W. J. Kelvin Chew, and W.D. Teng, Ceram. Int. 34 (2008) 1603-1608.
15. S. Ramesh, Z.Z. Loo, C.Y. Tan, W.J.K. Chew, Y.C. Ching, F. Tarlochan, H. Chandran, S. Krishnasamy, L.T. Bang, and A.A.D. Sarhan, Ceram. Int. 44 (2018) 10525-10530.
16. N.A.I.M. Razali, S. Pramanik, N.A. Abu Osman, Z. Radzi, and B. Pingguan-Murphy, J. Ceram. Process. Res. 17 (2016) 699-706.
17. C.K.L. Jeffrey, S. Ramesh, C.Y. Tan, and W.D. Teng, J. Ceram. Process. Res. 17 (2016) 620-625.
18. M.H. Bae, J.K. Kim, and S.C. Ryu, J. Ceram. Process. Res. 17 (2016) 518-522.
19. S. Ramesh, C.K.L. Jeffrey, C.Y. Tan, Y.H. Wong, P. Ganesan, S. Ramesh, M.G. Kutty, H. Chandran, and P. Devaraj, Ceram. Int. 42 (2016) 15756-15761.
20. E.J. Lee, D.H. Kwak, and D.J. Kim, J. Ceram. Process. Res. 16 (2015) 330-334.
21. I.Y. Kim, S.B. Cho, and C. Ohtsuki, J. Ceram. Process. Res. 15 (2014) 474-479.
22. L.-l. Wang, X.-F. Wang, C.-L. Yu, and Y.-Q. Zhao, J. Ceram. Process. Res. 14 (2013) 700-702.
23. B.-H. Kang, S.C. Ryu, and H.C. Park, J. Ceram. Process. Res.13 (2012) 791-796.
24. F. Liu, K. Zhou, and Z. Li, J. Ceram. Process. Res. 12 (2011) 567-571.
25. S. Ramesh, A.N. Natasha, C.Y. Tan, L.T. Bang, A. Niakan, J. Purbolaksono, Hari Chandran, C.Y. Ching, S. Ramesh, and W.D. Teng, Ceram. Int. 41 (2015) 10434-10441.
26. S. Ramesh, C.Y. Tan, C.L. Peralta, and W.D. Teng, Sci. Tech. Adv. Mater. 8 (2007) 257-263.
27. C. Bowen, S. Ramesh, C. Gill, and S. Lawson, J. Mater. Sci. 33 (1998) 5103-5110.
28. S. Ramesh, N. Zulkifli, C.Y. Tan, Y.H. Wong, F. Tarlochan, S. Ramesh, W.D. Teng, I. Sopyan, L.T. Bang, and A.A.D. Sarhan, Ceram. Int. 44 (2018) 8922-8927.
29. S. Ramesh, M. Amiriyan, S. Meenaloshini, R. Tolouei, M. Hamdi, J. Purboloksono, and W.D. Teng, Ceram. Int. 37 (2011) 3583-3590.
30. H. Misran, R. Singh, and M.A. Yarmo, Microporous and Mesoporous Mater. 112 (2008) 243-253.
31. S. Ramesh, and C. Gill, Ceram. Int. 27 (2001) 705-711.
32. U. Sutharsini, M. Thanihaichelvan, C.H. Ting, S. Ramesh, C.Y. Tan, Hari Chandran, Ahmed A.D. Sarhan, S. Ramesh, and I. Urriés, Ceram. Int. 43 (2017) 7594-7599.
33. M. Afshar-Mohajer, A. Yaghoubi, S. Ramesh, A.R. Bushroa, K.M.C. Chin, C.C. Tin, and W.S. Chiu, Appl. Surf. Sci. 307 (2014) 1-6.
34. M.K.G. Abbas, S. Ramesh, K.Y. Sara Lee, Y.H. Wong, P. Ganesan, S. Ramesh, U. Johnson Alengaram, W.D. Teng, and J. Purbolaksono, Ceram. Int. 46 (2020) 27539-27549.
35. S. Ramesh, K.Y. Sara Lee, and C.Y. Tan, Ceram. Int. 44 (2018) 20620-20634.
36. D.H. Kwak, S.J. Hong, D.J. Kim, and P. Greil, J. Ceram. Process. Res. 11 (2010) 170-172.
37. A.N. Cormack and A. Tilocca, Philosophical Trans. Royal Soc. A - Mathematical Phys. Eng. Sci. 370 (2012) 1271-

1280.
38. C.Y. Tan, A. Yaghoubi, S. Ramesh, S. Adzila, J. Purbolaksono, M.A. Hassan, and M.G. Kutty, Ceram. Int. 39 (2013) 8979-8983.
39. S. Ramesh, C.Y. Tan, W.H. Yeo, R. Tolouei, M. Amiriyan, I. Sopyan, and W.D. Teng, Ceram. Int. 37 (2011) 599-606.
40. C.Y. Tan, R. Singh, Y.C. Teh, Y.M. Tan, and B.K. Yap, Int. J. Appl. Ceram. Tech. 12 (2015) 223-227.
41. V.K. Mishra, S.B. Rai, B.P. Asthana, O. Parkash, and D. Kumar, Ceram. Int. 40 (2014) 11319-11328.
42. A. Farzadi, M. Solati-Hashjin, F. Bakhshi, and A. Aminian, Ceram. Int. 37 (2011) 65-71.
43. M.H. Nazarpak, M. Solati-Hashjin, and F. Moztarzadeh, J. Ceram. Proc. Res. 10 (2009) 54-57.
44. J. Klinkaewnarong, E. Swatsitang, C. Masingboon, S. Seraphin, S. Maensiri, Current Appl. Phys. 10 (2010) 521-525.
45. P. Kamalanathan, S. Ramesh, L.T. Bang, A. Niakan, C.Y. Tan, J. Purbolaksono, H. Chandran, and W.D. Teng, Ceram. Int. 40 (2014) 16349-16359.
46. M.A. Roudan, S. Ramesh, A. Niakan, Y.H. Wong, M.A. Zavareh, H. Chandran, W.D. Teng, N. Lwin, and U. Sutharsini, J. Ceram. Process. Res. 18 (2017) 69-72.
47. M. Ozawa and S. Suzuki, J. Am. Ceram. Soc. 85 (2002) 1315-1317.
48. D.S. Seo, K.H. Hwang, S.Y. Yoon, and J.K. Leed, J. Ceram. Process. Res. 13 (2012) 586-589.
49. M.E. Bahrololoom, M. Javidi, S. Javadpour, and J. Ma, J. Ceram. Process. Res. 10 (2009) 129-138.
50. A. Niakan, S. Ramesh, P. Ganesan, C.Y. Tan, J. Purbolaksono, H. Chandran, S. Ramesh, and W.D. Teng, Ceram. Int. 41 (2015) 3024-3029.
51. C.Y. Ooi, M. Hamdi, and S. Ramesh, Ceram. Int. 33 (2007) 1171-1177.
52. G.S. Kumar, A. Thamizhavel, and E.K. Girija, Mater. Letts. 76 (2012) 198-200.
53. W.F. Ho, H.C. Hsu, S.K. Hsu, C.W. Hung, and S.C. Wu, Ceram. Int. 39 (2013) 6467-6473.
54. G.S. Kumar, and E.K. Girija, Ceram. Int. 39 (2013) 8293-8299.
55. M. Akram, R. Ahmed, I. Shakir, W.A.W. Ibrahim, and R. Hussain, J. Mater. Sci. 49 (2014) 1461-1475.
56. S. Ramesh, A.N. Natasha, C.Y. Tan, L.T. Bang, S. Ramesh, C.Y. Ching, and H. Chandran, Ceram. Int. 42 (2016) 7824-7829.
57. T.S. Kang, C.M. Pantilimon, and S.J. Lee, J. Korean Ceram. Soc. 52 (2015) 204-208.
58. S.M. Naga, H.F. El-Maghraby, M. Sayed, and E.A. Saad, J. Ceram. Sci. Tech. 6 (2015) 237-243.
59. S. Ramesh, S. Adzila, C.K.L. Jeffrey, C.Y. Tan, J. Purbolaksono, A.M. Noor, M.A. Hassan, I. Sopyan, and W.D. Teng, J. Ceram. Process. Res. 14 (2013) 448-452.
60. S.C. Wu, H.K. Tsou, H.C. Hsu, S.K. Hsu, S.P. Liou, and W.F. Ho, Ceram. Int. 39 (2013) 8183-8188.
61. S. Jadalannagari, S. More, M. Kowshik, and S.R. Ramanan, Mater. Sci. Eng. C 31 (2011) 1534-1538.
62. G. Gergely, F. Weber, I. Lukacs, A.L. Toth, Z.E. Horvath, J. Mihaly, and C. Balazsi, Ceram. Int. 36 (2010) 803-806.
63. S.C. Wu, H.C. Hsu, S.K. Hsu, Y.C. Chang, and W.F. Ho, J. Asian Ceram. Soc. 4 (2016) 85-90.
64. K.P. Sanosh, M.C. Chu, A. Balakrishnan, T.N. Kim, and S.J. Cho, Mater. Letts. 63 (2009) 2100-2102.
65. Y.Z. Wang, and Y. Fu, Mater. Letts. 65 (2011) 3388-3390.
66. R.P. Singh, M.S. Mehta, S. Shukla, S. Singh, S. Singh, and R. Verma, J. Sol-Gel Sci. Tech. 84 (2017) 332-340.
67. S.A. Poursamar, M. Rabiee, A. Samadikuchaksaraei, M. Tahriri, M. Karimi, and M. Azami, J. Ceram. Process. Res. 10 (2009) 679-682.
68. S. Jalota, A.C. Tas, and S.B. Bhaduri, J. Mater. Res. 19 (2004) 1876-1881.
69. V.K. Mishra, S.K. Srivastava, B.P. Asthana, and D. Kumar, J. Am. Ceram. Soc. 95 (2012) 2709-2715.
70. D.E. Wagner, J. Lawrence, and S.B. Bhaduri, J. Mater. Res. 28 (2013) 3119-3129.
71. Y. Tanaka, Y. Hirata, and R. Yoshinaka, J. Ceram. Process. Res. 4 (2003) 197-201.
72. J.S. Cho, D.S. Jung, J.M. Han, and Y.C. Kang, J. Ceram. Process. Res. 9 (2008) 348-352.
73. A. Lak, M. Mazloumi, M.S. Mohajerani, S. Zanganeh, M.R. Shayegh, A. Kajbafvala, H. Arami, and S.K. Sadrnezhaad, J. Am. Ceram. Soc. 91 (2008) 3580-3584.
74. N. Bovanda, S. Rasoulib, M.-R. Mohammadic, and D. Bovandd, J. Ceram. Process. Res. 13 (2012) 221-225.
75. A. Siddharthan, T.S.S. Kumar, and S.K. Seshadri, Biomed. Mater. 4 (2009) 045010.
76. K.W. Goh, Y.H. Wong, S. Ramesh, H. Chandran, S. Krishnasamy, A. Sidhu, and W.D. Teng, Ceram. Int. 47 (2021) 8879-8887.
77. V. Apalangya, V. Rangari, S. Jeelani, E. Dankyi, A. Yaya, and S. Darko, Ceram. Int. 44 (2018) 7165-7171.
78. Z.W. Yang, Y.S. Jiang, Y.J. Wang, L.Y. Ma, and F.F. Li, Mater. Letts. 58 (2004) 3586-3590.
79. R. Nazir, N. Iqbal, A.S. Khan, A. Akram, A. Asif, A.A. Chaudhry, I.U. Rehman, and R. Hussain, Ceram. Int. 38 (2012) 457-462.
80. K. Hetherin, S. Ramesh, and Y.H. Wong, J. Mater. Sci.-Mater. Elect. 28 (2017) 11994-12003.
81. K. Hetherin, S. Ramesh, and Y.H. Wong, Appl. Phys. A 123 (2017) 510.
82. G.K. Williamson and W.H. Hall, Acta Metallurgica 1 (1953) 22-31.
83. U. Sabu, G. Logesh, M. Rashad, A. Joy, and M. Balasubramanian, Ceram. Int. 45 (2019) 6718-6722.
84. S.H. Jhung, T. Jin, Y.K. Hwang, and J.S. Chang, Chem. Eur. J. 13 (2007) 4410-4417.
85. L. Li, Y.K. Liu, J.H. Tao, M. Zhang, H.H. Pan, X.R. Xu, and R.K. Tang, J. Phys. Chem. C 112 (2008) 12219-12224.
86. S. Koutsopoulos, J. Biomed. Mater. Res. 62 (2002) 600-612.
87. J. Vandiver, D. Dean, N. Patel, C. Botelho, S. Best, J.D. Santos, M.A. Lopes, W. Bonfield, and C. Ortiz, J. Biomed. Mater. Res. A 78 (2006) 352-363.
88. Y. Fujishiro, H. Yabuki, K. Kawamura, T. Sato, and A. Okuwaki, J. Chem. Tech. Biotech. 57 (1993) 349-353.